Annals of Glaciology

Retreat and volume loss of two rapidly vanishing Svalbard glaciers since 1938: Elsabreen and Ferdinandbreen, Petuniabukta

Rebecca McCerery[1], Harold Lovell[2], Owen King[3], Bethan J. Davies[3], Jakub Małecki[4], Clare Boston[2], John Woodward[1] and Jonathan L. Carrivick[5]

[1]School of Geography and Natural Sciences, Northumbria University, Newcastle upon Tyne, UK; [2]School of the Environment and Life Sciences and Institute of the Earth and Environment, University of Portsmouth, Portsmouth, UK; [3]School of Geography, Politics and Sociology, Newcastle University, Newcastle upon Tyne, UK; [4]Institute of Geoecology and Geoinformation, Adam Mickiewicz University, Poznań, Poland and [5]School of Geography and Water@Leeds, University of Leeds, Leeds, UK

Letter

Cite this article: McCerery R, Lovell H, King O, Davies BJ, Małecki J, Boston C, Woodward J, Carrivick JL (2026) Retreat and volume loss of two rapidly vanishing Svalbard glaciers since 1938: Elsabreen and Ferdinandbreen, Petuniabukta. *Annals of Glaciology* **67**, e3, 1–10. https://doi.org/10.1017/aog.2025.10034

Received: 27 June 2025
Revised: 3 November 2025
Accepted: 10 December 2025

Keywords:
climate change; glacier retreat; Svalbard; vanishing glacier

Corresponding author: Rebecca McCerery; Email: r.mccerery@northumbria.ac.uk

Abstract

The Arctic is one of the fastest-warming places on Earth. The High Arctic Archipelago of Svalbard contains over 1500 glaciers that have, overall, experienced widespread thinning and recession since the Little Ice Age (LIA; ~1900 CE), and this recession has accelerated since 1990. Here, we showcase the terminal decline since the end of the LIA of Elsabreen and Ferdinandbreen, two small land-terminating glaciers in Petuniabukta, Dickson Land. We map glacier areal extents using previously published data, aerial photographs and satellite imagery (LIA to 2024) and derive ice volume changes by differencing digital elevation models (1938 to 2023). Both glaciers have lost over 93% of their glacier area since the LIA and over 96% of their ice volume since 1938. By 2024, Elsabreen had reduced to a small glacier remnant with little evidence of ice flow, and Ferdinandbreen had fragmented into several separate ice units and completely detached from its original accumulation areas. Both of these vanishing glaciers merit inclusion on the Global Glacier Casualty List.

1. Introduction

The Svalbard archipelago, located in the Barents Sea, is among the world's most climate-sensitive regions (Serreze and Barry, 2011; Isaksen and others, 2016; Nordli and others, 2020; Geyman and others, 2022). Its glaciers are particularly vulnerable to rising temperatures due to their relatively low elevation and Svalbard's position on the outer margins of the North Atlantic warm current (Nuth and others, 2010). Since the Little Ice Age (LIA) at around 1900 CE, when many of Svalbard's glaciers reached their maximum Neoglacial positions, glacier cover across the archipelago has decreased by around 13% (Nuth and others, 2013; Martín-Moreno and others, 2017; Mannerfelt and others, 2024).

Recent warming has caused Svalbard's mean annual air temperature to rise approximately 1.7°C per decade since 1991—seven times the global average (Nordli and others, 2020). Svalbard's location on the edge of the warm Atlantic Waters further adds to the archipelago's vulnerability, bringing heat to the Arctic Ocean through the Fram Strait (Schauer and others, 2004; Promińska and others, 2017). These warm ocean waters carried by the West Spitsbergen Current are consequently warming the fjords, affecting sea ice coverage (Muckenhuber and others, 2016), and have been attributed to accelerated rates of frontal ablation of Svalbard's marine-terminating glaciers (Li and others, 2025). This rapid warming and sensitivity to the warm Atlantic waters are significantly impacting glacier mass balance and accelerating glacial thinning and retreat across the region (Schuler and others, 2020; Geyman and others, 2022). Under current climatic projections, van Pelt and others (2021) project that the climatic mass balance (CMB), the total net change in glacier mass, for all Svalbard glaciers will become negative by 2060. A negative CMB causes equilibrium line altitudes to rise above the highest elevations of a glacier, resulting in enhanced mass loss and glacier recession.

For many land-terminating glaciers, thinning leads to fragmentation into smaller isolated units (e.g. Jiskoot and Mueller, 2012), as has already been documented across Svalbard (Małecki, 2016; Mannerfelt and others, 2024; McCerery and others, 2025), the European Alps (Paul and others, 2004; Cossart and Fort, 2008), the Juneau Icefield, Alaska (Davies and others, 2022, 2024), the Clemenceau Icefield, Canada (Jiskoot and others, 2009; Rippin and others, 2020), Greenland (Carrivick and others, 2019, 2023; Grimes and others, 2024), the Southern Alps of

New Zealand (Carrivick and others, 2020), across the Andes (Carrivick and others, 2024) and in the Himalaya (Lee and others, 2021; Rowan and others, 2021). Several of these studies have demonstrated that ice masses that become detached from parent accumulation areas decay at an accelerated rate compared with neighbouring glaciers that remain connected (Jiskoot and others, 2009; Paul and others, 2004; Jiskoot and Mueller, 2012). This highlights the importance of this stage in the glacier lifecycle in the context of glacier preservation in a warming climate and, in particular, the documentation of "vanishing" glaciers as well as the Global Glacier Casualty List (Boyer and Howe, 2024).

Svalbard's rapidly retreating glaciers and their particular sensitivity to climate change make them an ideal natural laboratory for understanding the state and fate of glaciers under accelerated warming. Small glaciers like those presented here are common in Svalbard and may be most vulnerable to climate change. The two glaciers studied here, Ferdinandbreen and Elsabreen, were 1.32 and 0.16 km^2 in size in 2009, respectively. According to the Randolph Glacier Inventory 7.0 Consortium 2023 (RGI 7.0 consortium, 2023) (see GLIMS: Global Land Ice Measurements from Space), there were 755 glaciers of a similar size or smaller than Ferdinandbreen and 118 glaciers of a similar size or smaller than Elsabreen in the year 2000. Here, we document the recession and thinning of these two vanishing glaciers, Elsabreen and Ferdinandbreen since the LIA. We use aerial photographs and satellite imagery to map historical glacier extents and multitemporal digital elevation models (DEMs) to reconstruct glacier volume changes over time. These are just two examples of rapidly retreating and thinning small glaciers on Svalbard.

2. Study sites

Elsabreen (78°40′ N, 16°22′ E) and Ferdinandbreen (78°42′ N, 16°18′ E) are neighbouring land-terminating glaciers located in Petuniabukta at the northern end of Billefjorden, Spitsbergen (Fig. 1). Both glaciers were historically polythermal valley glaciers, but now only small ice remnants or fragments remain (Rachlewicz and others, 2007; Kavan and Haagmans, 2021). More recent ice depth investigations using ground penetrating radar (GPR) and analyses of ice surface characteristics indicate both Elsabreen and Ferdinandbreen are now too thin to sustain polythermal conditions and have transitioned into a cold-based thermal regime (Małecki, 2013; Mallinson, 2019; Procházková and others, 2019; Kavan and Haagmans, 2021). Kavan and Haagmans (2021) suggest there are three key factors driving recently observed thinning patterns: (i) continued increasing air temperatures, (ii) low precipitation and (iii) topographic risk factors affecting shading and solar radiation exposure.

Ferdinandbreen is the northernmost of the two glaciers and is located on an east facing slope. The surrounding landscape is composed of ice-cored moraine, thin debris stripes and till cover (Evans and others, 2012; McCerery and others, 2024, 2025). Ferdinandbreen's historical polythermal conditions are evidenced by relict meltwater channels and abandoned glaciofluvial outwash plains that extend down valley to the LIA moraine sequence (McCerery and others, 2024, 2025). Since the LIA, Ferdinandbreen has lost over 90% of its clean ice area and ice volume (Table 1) (Rachlewicz and others, 2007; Procházková and others, 2019; Kavan, 2020). Its LIA position is delimited by a prominent latero-frontal moraine system, and the ice front was likely ~50 m thick at this time (Kavan, 2020). Ferdinandbreen had a maximum ice thickness of 42.1 m in 2014 based on GPR surveys and is currently believed to be cold-based (Procházková and others, 2019) but likely had areas of temperate ice when it was thicker and more extensive during the LIA.

Elsabreen is located in the adjacent valley, approximately 2 km south of Ferdinandbreen, within the cirque on the northern side of Pyramiden (937 m elevation) on a north-facing slope. Elsabreen also hosts evidence of previous polythermal conditions, with relict meltwater channels extending down valley but with no indications of a current subglacial hydrological system, i.e., active meltwater channels or presence of subglacial bedforms. Elsabreen is also estimated to have lost substantial amounts of its clean ice area and ice volume since the LIA (Table 1) (Rachlewicz and others, 2007; Procházková and others, 2019). The glacier had a maximum ice thickness of ~50 m in 2015 based on GPR surveys and is likely to be entirely cold-based today (Procházková and others, 2019).

3. Data and methods

Glacier areal extents since the LIA were mapped digitally in ArcGIS Pro (version 3.3.0) from previously published glacier outlines, aerial photographs and satellite images. The LIA extent was based on the prominent LIA latero-frontal moraine limits, as identified on the Norwegian Polar Institute (NPI) 2009 aerial photographs. The 1938 glacier extents are from Geyman and others (2022), based on NPI oblique aerial photographs. Glacier outlines in 1960–1990 were taken from Małecki (2013), who mapped them from an NPI topographic map and aerial photographs, respectively. The 2009 extents were mapped from NPI aerial photographs accessed from TopoSvalbard (https://toposvalbard.npolar.no/). Satellite imagery was used to map glacier outlines in 2013 (Landsat 7 ETM + image, captured 13 July 2013), 2021 (ArcGIS Pro Basemap imagery), 2023 and 2024 (Sentinel-2 imagery captured 2 August 2023 and 9 August 2024, respectively). Glacier areal extent uncertainty was calculated following the approach of Małecki (2016) and Geyman and others (2022): buffers corresponding to the reported spatial resolution (pixel size) of the source data were applied to each mapped outline. The following buffers were used: LIA = ±50 m, 1938 = ±5 m, 1960 = ±25 m, 1990 = ±10 m, 2009 = ±2 m, 2013 = ±30 m, 2021 = ±5 m, and 2023 and 2024 = ±10 m. The difference between the areas of the originally mapped glacier outline and the buffered glacier outline was then calculated, and this value was reported as the uncertainty. To estimate glacier volume change, we examined DEMs generated from optical stereo images acquired during regional aerial photography surveys and by contemporary satellites. The earliest DEM in our time series is that generated by Geyman and others (2022), who reconstructed surface elevations across Svalbard from oblique image surveys conducted in 1936 and 1938, the latter of which covers the area around Ferdinandbreen and Elsabreen. We also use DEMs generated from vertical aerial photographs acquired in 1990 and 2009 by the NPI, and we incorporate two ArcticDEM strips (Porter and others, 2022) generated from images acquired on 6 May 2013 and 19 May 2023 by the Worldview 2/3 satellites.

To generate robust estimates of glacier surface elevation and therefore glacier volume change, sequential DEMs must have consistent geolocation and be devoid of spatial biases, which can impact derived elevation change rates if left untreated. To coregister the DEMs from different timesteps, we first resample all to a common resolution (20 m, matching the lowest resolution 1990 DEM) using a bilinear interpolation approach. We follow established DEM coregistration methods (Nuth and Kääb, 2011) implemented in xDEM (xDEM contributors, 2025, https://zenodo.org/records/

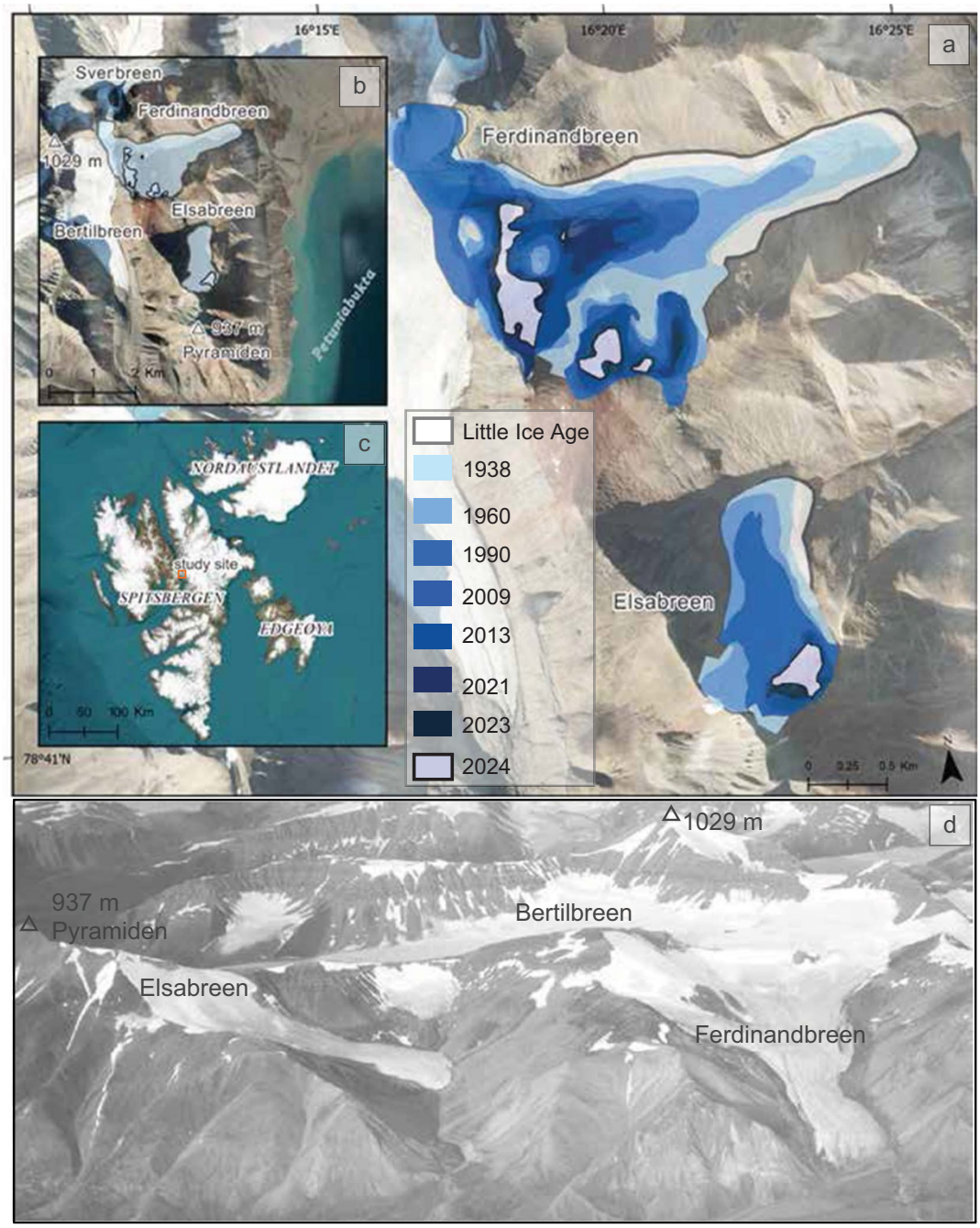

Figure 1. (a) Elsabreen and Ferdinandbreen areal extents from LIA to 2024. (b) Location of Elsabreen, Ferdinandbreen and neighbouring Bertilbreen in Petuniabukta. The LIA and 2024 extents of Elsabreen and Ferdinandbreen are shown. (c) Study area location (Orange box) within Spitsbergen, Svalbard. Background satellite imagery sourced from ESRI basemap imagery (2021). (d) 1938 oblique aerial photograph of Elsabreen and Ferdinandbreen sourced from the Norwegian Polar Institute TopoSvalbard archive (photograph ID: S38_2784).

11492983) to remove horizontal shifts in *x, y* and *z* directions. Mean values of stable ground (off-glacier) elevation change differences are shown in Table 2, which should be negligible when DEM coregistration has been successful.

To derive volume change over different time periods between DEM dates, we multiply the mean value of elevation change (dH) by the area of each glacier at the initial date of each timestep. To estimate the portion of each glacier's total volume lost through time, we treat the 2023 DEM as representative of ice-free conditions, given the small remaining volume of each glacier at this point in time (Fig. 1). We therefore treat the ice volume lost from 1938 to 2023 as 100% of each glacier's total volume over our study period, with ice lost over intermediate timesteps subtracted from this total volume to derive the relative contribution of each sub-period to total volume change.

We follow the methods of Hugonnet and others (2022) to estimate the uncertainty associated with elevation change data we derived across different time periods. This method, also implemented in xDEM, examines and models how the vertical precision of DEMs varies spatially considering different terrain metrics

Table 1. Summary of ice loss for Ferdinandbreen and Elsabreen from previous works.

Year	Ferdinandbreen change	Reference
LIA to 2005	43.9% loss of clean ice area	Rachlewicz and others, 2007
1990 to 2015	48.1% of ice volume	Procházková and others, 2019
1938 to 2014	92.5% of ice volume	Kavan, 2020
Year	**Elsabreen change**	**Reference**
LIA to 2005	53.5% loss of clean ice area	Rachlewicz and others, 2007
1990 to 2015	74.2% of ice volume	Procházková and others, 2019

Table 2. Mean and normalised median absolute deviation (NMAD) of stable ground (off-glacier) covered by each of the different elevation change datasets derived from sequential DEMs. AP refers to DEMs generated from aerial photography.

DEM pair	Off-glacier mean dH/NMAD (m)
1936 (AP) to 2023 (ArcticDEM)	−0.84/3.20
1936 (AP) to 1990 (AP)	0.95/3.39
1990 (AP) to 2009 (AP)	−0.42/2.13
2009 (AP) to 2013 (ArcticDEM)	0.18/0.87
2013 (ArcticDEM) to 2023 (ArcticDEM)	0.39/1.14

(slope, curvature) and how DEM errors correlate over different domains. Estimated elevation change rate uncertainties range between ± 0.04 and 0.32 m a^{-1} and are generally much lower than the magnitude of elevation changes measured over Ferdinandbreen and Elsabreen. Volume change uncertainty is calculated as the elevation change uncertainty multiplied by glacier area at the beginning of each timestep. To estimate the uncertainty associated with our calculated total glacier volumes at each timestep, we propagate our elevation change uncertainty with an estimate of glacier area uncertainty (5% of glacier area at each timestep), assuming the two are independent.

4. Results

Since the LIA, Elsabreen and Ferdinandbreen have undergone extensive and continuous recession and thinning (Figs. 1 and 2). Based on moraine positions, Elsabreen and Ferdinandbreen had areal extents of 0.9 and 2.9 km^2 at the LIA, respectively. By 1990, both glaciers had lost almost half of their LIA surface area and approximately two-thirds of their ice volume compared to their 1938 thicknesses (Table 3). In total, Elsabreen has lost 93.3% of its area (LIA to 2024) and 96.0% of its ice volume (1938–2023). Ferdinandbreen has lost 93.7% of its area (LIA to 2024) and 99.7% of its volume (1938–2023). Between 1938 and 2023, Elsabreen underwent a mean surface elevation lowering of 29.9 ± 3.1 m, and Ferdinandbreen experienced a mean surface elevation lowering of 31.4 ± 3.5 m (Table 3). The highest rate of volume change for both glaciers occurred from 1990 to 2009 (Ferdinandbreen: 1 million m^3 a^{-1}; Elsabreen: 0.3 million m^3 a^{-1}), closely followed by similar volume change rates between 1938 and 1990. Since 2009, Ferdinandbreen's rate of volume change has halved, and Elsabreen's has reduced by two-thirds. Ferdinandbreen's surface lowering rate was highest in 1990–2009 (−0.8 ± 0.1 m a^{-1}) and has remained higher between 2009 and 2013 (−0.6 ± 0.3 m a^{-1}) and 2013 and 2023 (−0.5 ± 0.1 m a^{-1}) than the period from 1938 to 1990 (−0.4 ± 0.06 m a^{-1}) (Fig. 3a). Elsabreen has experienced the highest rates of surface lowering between 2013 and 2023 (−0.7 ± 0.1 m a^{-1}), broadly comparable to that experienced between 1990 and 2009 (−0.6 ± 0.1 m a^{-1}) and approximately double the surface lowering rates between 1938 and 1990 (−0.3 ± 0.06 m a^{-1}) and 2009 and 2013 (−0.2 ± 0.2 m a^{-1}) (Fig. 3a).

Throughout post-LIA recession and thinning, Elsabreen has largely remained as a single consistent ice mass, albeit by 2024 heavily restricted to a small ice remnant in the higher elevations on the eastern side of the cirque (Figs. 1 and 4). The glacier had a mean ice thickness of 21.2 ± 0.8 m in 2015 (Procházková and others, 2019) and has since lost over half of its ice volume (2013–2023), suggesting the remaining ice is likely very thin. Ferdinandbreen also initially receded as a single ice mass, but by 1990, two bedrock bumps had begun to emerge from the thinning ice (Fig. 1). The continued emergence of the bedrock bumps from 2008 is shown in Fig. 5, demonstrating the rapid fragmentation of the main glacier tongue. The higher of the bedrock bumps separates Ferdinandbreen from neighbouring Bertilbreen. These two glaciers were contiguous throughout much of the period of study. However, by 2017/18, Ferdinandbreen had become almost entirely disconnected from Bertilbreen, consistent with the negligible ice thickness in this area and the overall mean ice thickness of 13.3 ± 0.8 m recorded by Procházková and others (2019) in 2014. The ice divide between Bertilbreen and Ferdinandbreen (Procházková and others, 2019) likely shifted eastwards and to lower elevations as the upper part of Ferdinandbreen thinned, until the point of complete disconnection from Bertilbreen sometime before 2021 (Fig. 5). By 2024, only a series of small, isolated and very thin, clean ice patches remained in Ferdinandbreen's ablation area (Figs. 1 and 5).

5. Discussion

Elsabreen and Ferdinandbreen have lost almost all (96–99.7%) of their LIA ice volume in a little over a century and, as of 2024, are very small, thin and likely entirely cold-based ice masses with little discernible ice flow (Rachlewicz and others, 2007; McCerery and others, 2025). Our ice volume change calculations are in general agreement with those presented by Procházková and others (2019) and Kavan (2020), who used GPR surveys and photogrammetry, respectively, to reconstruct geometric changes of the glaciers for parts of our study duration. Ferdinandbreen was calculated to have lost 92.6% of ice volume from 1908 to 2014 by Kavan (2020), compared to 99.7% from 1938 to 2023 in this study (Table 2). We demonstrate that Ferdinandbreen lost ice volume at the fastest rate between 1990 and 2009 (1.1 million m^3 a^{-1}) (Fig. 3b), whereas Kavan (2020) identified the highest rate of volume change between 1938 and 1960 (2.2 million m^3 a^{-1}). A step change in summer air temperatures and a decrease in winter snow accumulation from 1990 have been suggested to be responsible for enhanced thinning and recession after this time (James and others, 2012; Małecki, 2013, 2016), consistent with our observations from Elsabreen and Ferdinandbreen.

Procházková and others (2019) reconstructed volume changes of Elsabreen (1990–2015) and Ferdinandbreen (1990–2014) and concluded the glaciers lost 74.2% (Elsabreen) and 48.1% (Ferdinandbreen) of their ice volume over this period. The calculated loss for Elsabreen compares well to our ice volume loss calculations of 76.3% over a comparable time period between 1990 and 2013. We suggest the variations in volume changes for Ferdinandbreen from 1990 to 2013/2014, for which we calculate over twice as much volume loss (and 82.8%) compared to Procházková and others (2019), partly reflecting differences in the mapped extents of the glacier in 1990 between the studies. In

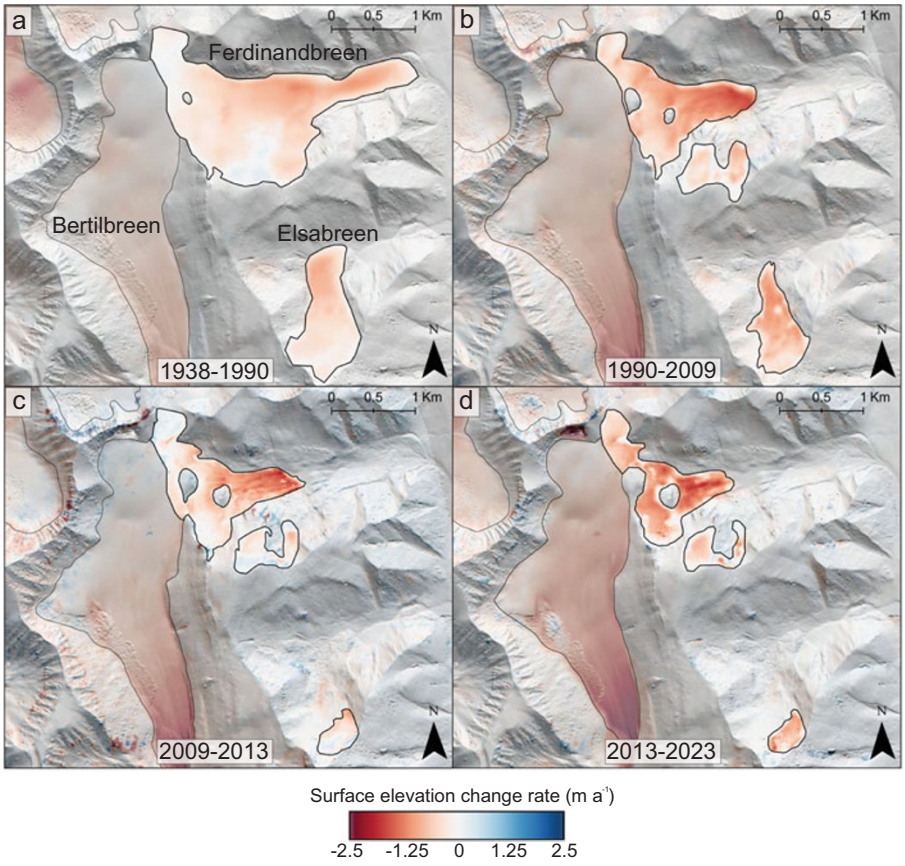

Figure 2. Elevation change rates (m a^{-1}) over Ferdinandbreen and Elsabreen between (a) 1938 and 1990, (b) 1990 and 2009, (c) 2009 and 2013 and (d) 2013 and 2023 with glacier outlines from 1990, 2009, 2013 and 2023, respectively.

Table 3. Elsabreen and Ferdinandbreen area and volume changes from LIA to 2024.

Glacier	Year	Area (km^2)	Volume (million m^3)	Volume (%)	ΔH (m)	ΔH period
Elsabreen	LIA	0.90 ± 0.23	-	-	-	-
	1938	0.80 ± 0.02	23.90 ± 2.77	100	−29.86 ± 3.10	1938–2023
	1960	0.70 ± 0.10	-	-	-	
	1990	0.49 ± 0.04	7.88 ± 1.82	32.99 ± 2.32	−20.01 ± 3.01	1936–1990
	2009	0.16 ± 0.00	1.90 ± 0.99	8.36 ± 4.95	−12.03 ± 2.10	1990–2009
	2013	0.13 ± 0.05	1.87 ± 0.27	7.83 ± 1.48	−0.81 ± 0.89	2009–2013
	2021	0.09 ± 0.00	-	-	-	
	2023	0.08 ± 0.02	0.95 ± 0.56	3.96 ± 0.59	−6.96 ± 1.14	2013–2023
	2024	0.06 ± 0.01	-	-	-	-
Ferdinandbreen	LIA	2.86 ± 0.48	-	-	-	-
	1938	2.55 ± 0.05	80.06 ± 8.92	100	−31.41 ± 3.50	1938–2023
	1960	1.96 ± 0.30	-	-	-	
	1990	1.47 ± 0.11	28.72 ± 5.03	35.88 ± 1.75	−20.14 ± 3.43	1936–1990
	2009	1.32 ± 0.03	7.83 ± 3.26	9.78 ± 4.17	−14.22 ± 2.47	1990–2009
	2013	1.02 ± 0.29	4.95 ± 1.32	6.18 ± 2.67	−2.18 ± 1.29	2009–2013
	2021	0.45 ± 0.04	-	-	-	
	2023	0.26 ± 0.06	0.26 ± 0.37	0.33 ± 1.43	−4.58 ± 1.42	2013–2023
	2024	0.18 ± 0.05	-	-	-	-

particular, we include the upper basin between Bertilbreen and Svenbreen in Ferdinandbreen's glacier outline up to 2013, after which this area becomes disconnected from Ferdinandbreen. We also include Ferdinandbreen's southern accumulation basin in our calculations throughout, which became detached from the main tongue by 1960 but still constitutes remnants of glacier ice within the Ferdinandbreen catchment (Fig. 1).

This central region of Spitsbergen is not only sensitive to the air and fjord temperature increases but also experiences relatively low amounts of yearly precipitation (previously described as a continental climate), which affects glacier mass balance and limits the amount of snow accumulation during the accumulation season (Przybylak and others, 2014; Gjelten and others, 2016; Kavan and Haagmans, 2021). Kavan and Haagmans's (2021) assessment of snow ablation on Elsabreen, Ferdinandbreen and neighbouring glaciers showed that only a small fraction of this already limited amount of snow that is deposited over winter persists into the summer ablation season. This results in large portions of the

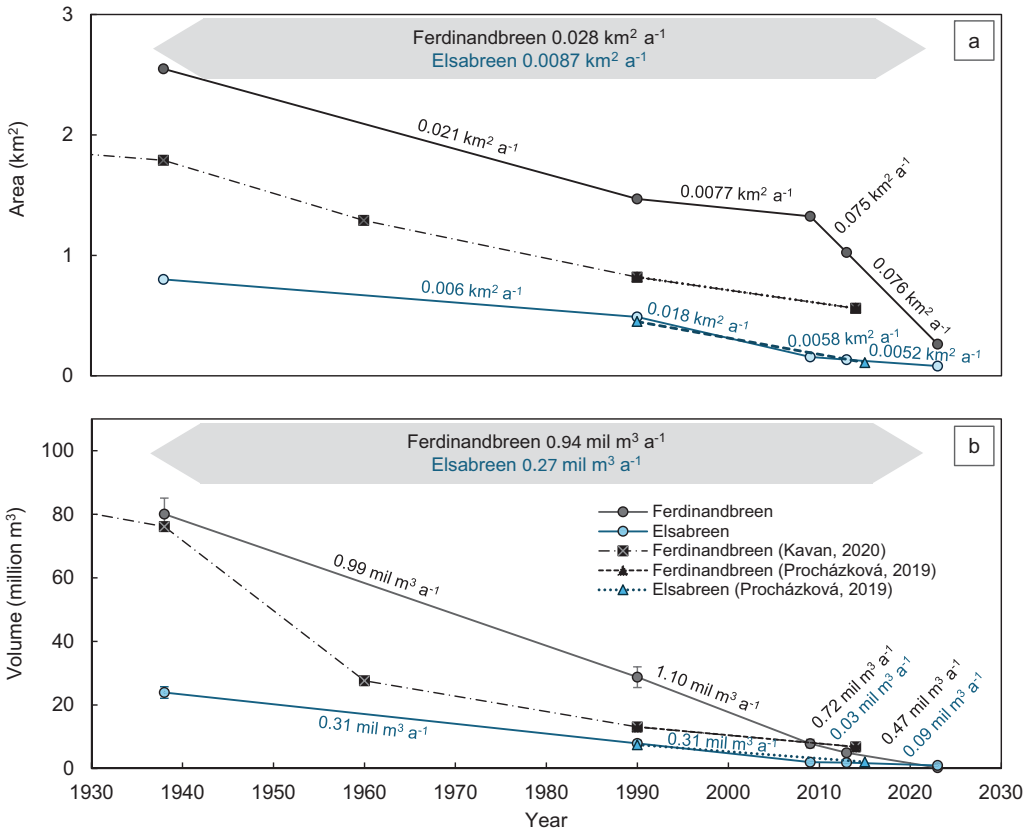

Figure 3. (a) Area change rates (km^2 a^{-1}) and (b) volume change rates (million m^3 a^{-1}) of Elsabreen and Ferdinandbreen between 1938 and 2023 with comparison to Procházková and others (2019) and Kavan (2020).

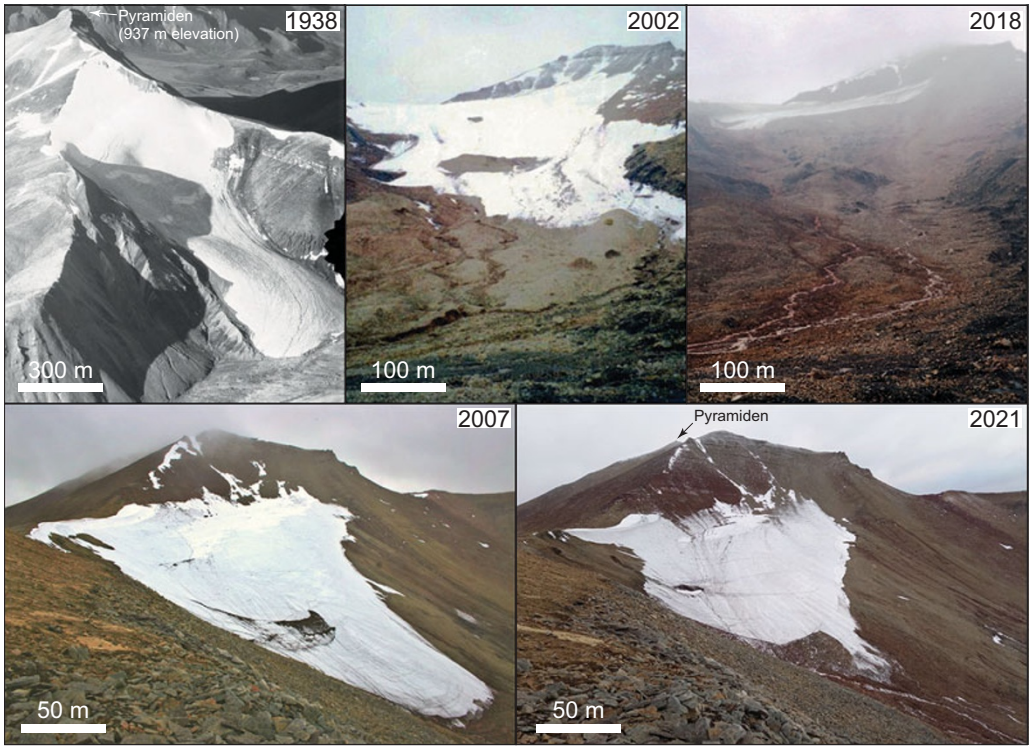

Figure 4. Elsabreen frontal recession and thinning from 1938 to 2021. The upper row shows a front-on view of the glacier in 1938 (image source from the Norwegian Polar Institute TopoSvalbard archive, photograph ID: S38_2705), 2002 (photograph taken by Witold Szczuciński) and 2018 (photograph taken by Jakub Małecki). The bottom row shows a side-on view of the glacier in 2007 and 2021 (both photographs taken by Jakub Małecki).

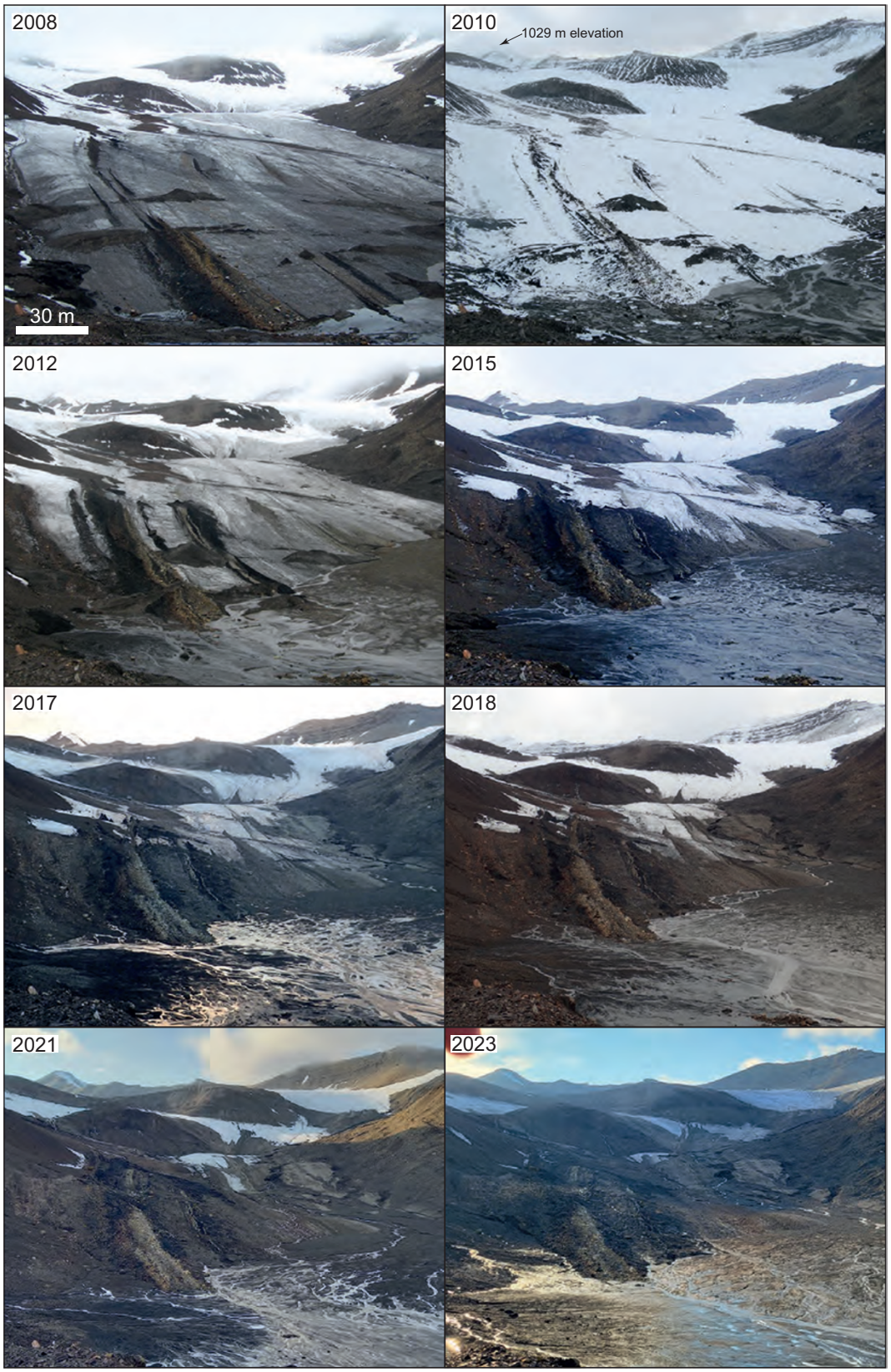

Figure 5. Ferdinandbreen frontal recession and thinning from 2008 to 2023 (all photographs taken by Jakub Małecki).

glacier surface experiencing snow-free cover, driving the glaciers into negative mass balance.

The demise of Elsabreen and Ferdinandbreen can be compared to other similar small land-terminating glaciers in Svalbard. In

Nordenskiöld Land, central Spitsbergen, Mannerfelt and others (2024) showed five glaciers, which in 1936 were slightly larger (2.7–4.7 km^2) than Ferdinandbreen in 1938 (2.5 km^2), lost on average 77.4 ± 7.7% of their ice volume between 1936 and 2019. One of which (Scott Turnerbreen) lost a comparable 91 ± 5% over this period. Also in Nordenskiöld Land, Aldegondabreen (9.5 km^2 in 1936) lost 73.1% of its ice volume between 1936 and 2016 (Holmlund, 2021). This magnitude of thinning is also especially striking when compared with the Geyman and others (2022) Svalbard-wide assessment of −14.8% glacier volume change from 1936/1938 to 2010. This dataset includes all glaciers ($n = 1594$), most of which are substantially larger than Elsabreen and Ferdinandbreen, thus highlighting the vulnerability to complete mass loss of these much smaller Svalbard glaciers.

Our data demonstrate that Ferdinandbreen has experienced more substantial ice volume loss in percentage terms since 2013 than Elsabreen (Table 2). This difference can be explained by the topographic context of both glaciers. Ferdinandbreen is underlain by at least two large bedrock bumps that have been emerging as the ice thinned since at least 1990. The upper bump is a ridge that now separates Ferdinandbreen from Bertilbreen (Fig. 4). As Ferdinandbreen has thinned, the main tongue has fragmented and a large bedrock outcrop now separates the two main units of the original glacier tongue. Once fragmentation was underway, the glacier receded at a faster rate due to positive feedback mechanisms. First, newly exposed bedrock surfaces drive enhanced radiative forcing to the surrounding thin ice (e.g. Wendler, 1975; Olyphant, 1986; Gratton and others, 1993; Hannah and others, 2000; Jiskoot and Mueller, 2012). Secondly, the fragmentation into smaller, thinner ice units and the complete disconnection from higher elevation accumulation areas lead to a reduction in ice flow (cf. Paul and others, 2004; Kargel and others, 2005; Jiskoot and Mueller, 2012; Rippin and others, 2020). These melt-accelerating feedbacks of fragmented ice represent a point of accelerating and irreversible glacier loss at Ferdinandbreen (e.g. Davies and others, 2024). By contrast, Elsabreen, whilst also in terminal decline, has maintained a single coherent ice mass and has been able to partially stabilise at a higher elevation within the more shaded eastern part of its cirque (Fig. 1). An additional factor is that by 2013, Elsabreen had already likely become too small to sustain the same pace of thinning rates (e.g. Małecki, 2013).

Our assessment of the future prognosis for Elsabreen and Ferdinandbreen is that their complete demise is likely imminent. By 2023, Ferdinandbreen had lost 99.7% of its 1938 ice volume, completely disconnected from the Bertilbreen source area and fragmented into four small separate ice units (Figs. 1, 2 and 4; Table 2). The recent pace of Ferdinandbreen's disintegration is particularly dramatic. Kavan (2020), based on observed changes up to 2014, suggested the glacier was likely to disappear within 30 years (i.e. ∼2050). Our data show that by 2023, Ferdinandbreen had already lost 94.8% of its 2013 ice volume and Elsabreen had lost 50.0% of its 2013 ice volume, suggesting both may disappear long before 2050. Thus, the examples of vanishing Elsabreen and Ferdinandbreen provide important long-term evidence of rapid thinning and recession of Svalbard glaciers under climate warming and represent the likely trajectory of many other small land-terminating glaciers on the archipelago.

Such rapid glacier retreat and thinning have important implications for the deglaciating landscape left behind. These areas were likely ice free during the Holocene thermal optimum, where the Arctic experienced amplified climate shifts by increased oceanic and atmospheric temperatures, along with a large portion of north and west Spitsbergen (Fjeldskaar and others, 2018; Farnsworth and others, 2024). These areas then reglaciated in the Late Holocene (∼4.2–4.0 ka BP) with most glaciers reaching their maximum extent at the LIA (Fjeldskaar and others, 2018). Similar deglaciated transitions can now be seen in Svalbard associated with contemporary warming and climate change. Ferdinandbreen's rapid post-LIA recession has been shown to drive the delivery of sediments to the coastal area, developing spit systems in Billefjorden (Strzelecki and others, 2018). As the Ferdinand valley and Elsa cirque become fully deglaciated, their geomorphology will transition to a landscape dominated by paraglacial processes and landforms such as talus, debris cones and fans with uncertain long-term stability (Ballantyne, 2008). Such geomorphological shifts are already being observed on Svalbard, with newly exposed coastal systems characterised by deltas, cliffs and tidal flats, such as at Brepollen, Hornsund (Strzelecki and others, 2020). Glacier retreat on the archipelago has already exposed nearly 1000 km of new coastline since the 1930s (Kavan and Strzelecki, 2023) and over 200 km since 2000 (Kavan and others, 2025). This landscape shift will also impact the wider ecosystems. A reduction in glacier meltwater and associated sediment and nutrient inputs into the fjord will see a reduction in fjord productivity, impacting specialised mammals and birds such as ringed and bearded seals and kittiwakes (Hartley and Fisher, 1936; Lydersen and others, 2014; Meire and others, 2017; Kavan and Strzelecki, 2023).

It is clear that both glaciers have surpassed a threshold by which they can be sustained by current accumulation and with continued temperature rises due to climate change, their complete loss in the coming years appears inevitable. Elsabreen and Ferdinandbreen are strong candidates for the Global Glacier Casualty List, and the projected continued climate warming will cause the disappearance of land-terminating glaciers in Svalbard. In the future, it is also likely that both glaciers could also be added to the list of extinct glaciers in the GLIMS Glacier Inventory.

6. Conclusions

Elsabreen and Ferdinandbreen in Petuniabukta, Svalbard, have undergone rapid retreat and thinning since the LIA (∼1900 CE), which has accelerated post-1990. Both glaciers lost over 93% of their area and over 96% of their ice volume over this period and should be considered within the category of vanishing glaciers. The highest rates of volume change occurred between 1990 and 2009, coincident with Ferdinandbreen beginning to fragment around a number of bedrock bumps. Glacier fragmentation processes were evidenced from 2008, leading to the glacier completely disconnecting from its higher elevation accumulation areas by 2021. In 2024, both Elsabreen and Ferdinandbreen were very small, thin and isolated ice remnants with likely only very limited ice flow, if any at all, and their longevity can be measured in years rather than decades. Based on our analysis, deglaciation of Elsabreen and Ferdinandbreen in the near future is inevitable, and the continued climate warming in Svalbard will likely mean many other thin and cold-based land-terminating glaciers will be joining them.

Data availability statement. Datasets of glacier outlines in .xshp format and DEMs of difference for Elsabreen and Ferdinandbreen created in this study are available on Zenodo at https://doi.org/10.5281/zenodo.17879675 and https://doi.org/10.5281/zenodo.17899856, respectively.

Acknowledgements. We would like to thank the staff and students at the Adam Mickiewicz University Polar Station in Petuniabukta for supporting fieldwork and the University of Portsmouth and Northumbria University for

fieldwork funding. We would also like to thank the two reviewers, Jan Kavan and an anonymous reviewer, scientific editor Hrafnhildur Hannesdottir and associate chief editor Liss Marie Andreassen for their comments that helped improve the manuscript.

References

Ballantyne CK (2008) After the ice: Holocene geomorphic activity in the Scottish Highlands. *Scottish Geographical Journal* **124**(1), 8–52. doi:10.1080/14702540802300167

Boyer D and Howe C (2024) *Global Glacier Casualty List*. August 17, 2024 doi:10.25613/CZJA-9V56

Carrivick JL and 7 others (2019) Accelerated volume loss in glacier ablation zones of NE Greenland, Little Ice Age to present. *Geophysical Research Letters* **46**(3), 1476–1484. doi:10.1029/2018GL081383

Carrivick JL and 4 others (2020) Ice thickness and volume changes across the Southern Alps, New Zealand, from the little ice age to present. *Scientific reports* **10**(1), 13392.

Carrivick JL and 10 others (2023) Mass loss of glaciers and ice caps across Greenland since the Little Ice Age. *Geophysical Research Letters* **50**(10), e2023GL103950. doi:10.1029/2023GL103950

Carrivick JL and 8 others (2024) Accelerating glacier area loss across the Andes since the Little Ice Age. *Geophysical Research Letters* **51**(13), e2024GL109154. doi:10.1029/2024GL109154

Cossart E and Fort M (2008) Sediment release and storage in early deglaciated areas: Towards an application of the exhaustion model from the case of Massif des Écrins (French Alps) since the Little Ice Age. *Norsk Geografisk Tidsskrift-Norwegian Journal of Geography* **62**(2), 115–131. doi:10.1080/00291950802095145

Davies B and 9 others (2022) Topographic controls on ice flow and recession for Juneau Icefield (Alaska/British Columbia). *Earth Surface Processes and Landforms* **47**(9), 2357–2390. doi:10.1002/esp.5383

Davies B and 9 others (2024) Accelerating glacier volume loss on Juneau Icefield driven by hypsometry and melt-accelerating feedbacks. *Nature Communications* **15**(1), 5099. doi:10.1038/s41467-024-49269-y

Evans DJ, Strzelecki M, Milledge DG and Orton C (2012) Hørbyebreen polythermal glacial landsystem, Svalbard. *Journal of Maps* **8**(2), 146–156. doi:10.1080/17445647.2012.680776

Farnsworth WR and 9 others (2024) Persistence of Holocene ice cap in northeast Svalbard aided by glacio-isostatic rebound. *Quaternary Science Reviews* **331**, 108625. doi: 10.1016/j.quascirev.2024.108625

Fjeldskaar W, Bondevik S and Amantov A (2018) Glaciers on Svalbard survived the Holocene thermal optimum. *Quaternary Science Reviews* **199**, 18–29. doi:10.1016/j.quascirev.2018.09.003

Geyman EC, van Pelt W, Maloof AC, Aas HF and Kohler J (2022) Historical glacier change on Svalbard predicts doubling of mass loss by 2100. *Nature* **601**(7893), 374–379. doi:10.1038/s41586-021-04314-4

Gjeltenf HM and 9 others (2016) Air temperature variations and gradients along the coast and fjords of western Spitsbergen. *Polar Research* **35**(1), 29878. doi: 10.3402/polar.v35.29878

Gratton DJ, Howarth PJ and Marceau DJ (1993) Using Landsat-5 Thematic Mapper and digital elevation data to determine the net radiation field of a mountain glacier. *Remote Sensing of Environment* **43**(3), 315–331. doi:10.1016/0034-4257(93)90073-7

Grimes M, Carrivick JL and Smith MW (2024) Spatial heterogeneity, terminus environment effects and acceleration in mass loss of glaciers and ice caps across Greenland. *Global and Planetary Change* **239**, 104505. doi:10.1016/j.gloplacha.2024.104505

Hannah DM, Gurnell AM and Mcgregor GR (2000) Spatio–temporal variation in microclimate, the surface energy balance and ablation over a cirque glacier. *International Journal of Climatology: A Journal of the Royal Meteorological Society* **20**(7), 733–758. doi:10.1002/1097-0088(20000615)20:7%3C733::AID-JOC490%3E3.0.CO;2-F

Hartley CH and Fisher J (1936) The marine foods of birds in an inland fjord region in west Spitsbergen: Part 2. Birds. *The Journal of Animal Ecology* 370–389. doi:10.2307/1041

Holmlund ES (2021) Aldegondabreen glacier change since 1910 from structure-from-motion photogrammetry of archived terrestrial and aerial photographs: Utility of a historic archive to obtain century-scale Svalbard glacier mass losses. *Journal of glaciology* **67**(261), 107–116. doi: 10.1017/jog.2020.89

Hugonnet R and 6 others (2022) Uncertainty analysis of digital elevation models by spatial inference from stable terrain. *IEEE Journal of Selected Topics in Applied Earth Observations and Remote Sensing* **15**, 6456–6472. doi: 10.1109/JSTARS.2022.3188922

Isaksen K, Nordli Ø, Førland EJ, Łupikasza E, Eastwood S and Niedźwiedź T (2016) Recent warming on Spitsbergen—Influence of atmospheric circulation and sea ice cover. *Journal of Geophysical Research: Atmospheres* **121**(20), 11–913. doi:10.1002/2016JD025606

James TD and 5 others (2012) Observations of enhanced thinning in the upper reaches of Svalbard glaciers. *The Cryosphere* **6**(6), 1369–1381. doi: 10.5194/tc-6-1369-2012

Jiskoot H, Curran CJ, Tessler DL and Shenton LR (2009) Changes in Clemenceau Icefield and Chaba Group glaciers, Canada, related to hypsometry, tributary detachment, length–slope and area–aspect relations. *Annals of Glaciology* **50**(53), 133–143. doi:10.3189/172756410790595796

Jiskoot H and Mueller MS (2012) Glacier fragmentation effects on surface energy balance and runoff: Field measurements and distributed modelling. *Hydrological Processes* **26**(12), 1861–1875. doi:10.1002/hyp.9288

Kargel JS and 10 others (2005) Multispectral imaging contributions to global land ice measurements from space. *Remote Sensing of Environment* **99**(1-2), 187–219. doi:10.1016/j.rse.2005.07.004

Kavan J (2020) Early twentieth century evolution of Ferdinand glacier, Svalbard, based on historic photographs and structure-from-motion technique. *Geografiska Annaler: Series A, Physical Geography* **102**(1), 57–67.

Kavan J and Haagmans V (2021) Seasonal dynamics of snow ablation on selected glaciers in central Spitsbergen derived from Sentinel-2 satellite images. *Journal of Glaciology* **67**(265), 961–966. doi:10.1017/jog.2021.36

Kavan J and Strzelecki MC (2023) Glacier decay boosts the formation of new Arctic coastal environments—Perspectives from Svalbard. *Land Degradation & Development* **34**(12), 3467–3474. doi:10.1002/ldr.4695

Kavan J, Szczypińska M, Kochtitzky W, Farquharson L, Bendixen M and Strzelecki MC (2025) New coasts emerging from the retreat of Northern Hemisphere marine-terminating glaciers in the twenty-first century. *Nature Climate Change* 1–10. doi:10.1038/s41558-025-02282-5

Lee E, Carrivick JL, Quincey DJ, Cook SJ, James WH and Brown LE (2021) Accelerated mass loss of Himalayan glaciers since the Little Ice Age. *Scientific Reports* **11**(1), 24284. doi:10.1038/s41598-021-03805-8

Li T and 6 others (2025) Pervasive glacier retreats across Svalbard from 1985 to 2023. *Nature Communications* **16**(1), 705. doi:10.1038/s41467-025-55948-1

Lydersen C and 10 others (2014) The importance of tidewater glaciers for marine mammals and seabirds in Svalbard, Norway. *Journal of Marine Systems* **129**, 452–471. doi:10.1016/j.jmarsys.2013.09.006

Małecki J (2013) Elevation and volume changes of seven Dickson Land glaciers, Svalbard, 1960–1990–2009. *Polar Research* **32**(1), 18400. doi:10.3402/polar.v32i0.18400

Małecki J (2016) Accelerating retreat and high-elevation thinning of glaciers in central Spitsbergen. *The Cryosphere* **10**(3), 1317–1329. doi:10.5194/tc-10-1317-2016

Mallinson L, Swift DA and Sole A (2019) Proglacial icings as indicators of glacier thermal regime: Ice thickness changes and icing occurrence in Svalbard. *Geografiska Annaler: Series A, Physical Geography* **101**(4), 334–349. doi:10.1080/04353676.2019.1670952

Mannerfelt ES, Hodson AJ, Håkansson L and Lovell H (2024) Dynamic LIA advances hastened the demise of small valley glaciers in central Svalbard. *Arctic Science* **10**(4), 815–833. doi:10.1139/as-2024-0024

Martín-Moreno R, Allende Alvarez F and Hagen JO (2017) 'Little Ice Age' glacier extent and subsequent retreat in Svalbard archipelago. *The Holocene* **27**(9), 1379–1390. doi:10.1177/095968361769390

McCerery R and 6 others (2025) Landsystem models from remote and field based geomorphological mapping reveal diverse glacier dynamics on svalbard. *Geomorphology* **484**, 109854. doi:10.1016/j.geomorph.2025.109854

McCerery R and 6 others (2024) Terrestrial glacial geomorphology of surge-type and non-surge-type glaciers on Svalbard. *Journal of Maps* **20**(1), 2362277. doi:10.1080/17445647.2024.2362277

Meire L and 8 others (2017) Marine-terminating glaciers sustain high productivity in Greenland fjords. *Global Change Biology* **23**(12), 5344–5357. doi:10.1111/gcb.13801

Muckenhuber S, Nilsen F, Korosov A and Sandven S (2016) Sea ice cover in Isfjorden and Hornsund, Svalbard (2000–2014) from remote sensing data. *The Cryosphere* **10**(1), 149–158. doi:10.5194/tc-10-149-2016

Nordli Ø and 6 others (2020) Revisiting the extended Svalbard Airport monthly temperature series, and the compiled corresponding daily series 1898–2018. *Polar Research* **39**(3614). doi:10.33265/polar.v39.3614

Nuth C and 7 others (2013) Decadal changes from a multi-temporal glacier inventory of Svalbard. *The Cryosphere* **7**, 1603–1621. doi: 10.5194/tc-7-1603-2013

Nuth C and Kääb A (2011) Co-registration and bias corrections of satellite elevation data sets for quantifying glacier thickness change. *The Cryosphere* **5**, 271–290. doi:10.5194/tc-5-271-2011

Nuth C, Moholdt G, Kohler J, Hagen JO and Kääb A (2010) Svalbard glacier elevation changes and contribution to sea level rise. *Journal of Geophysical Research: Earth Surface* **115**(F1). doi:10.1029/2008JF001223

Olyphant GA (1986) Longwave radiation in mountainous areas and its influence on the energy balance of alpine snowfields. *Water Resources Research* **22**(1), 62–66. doi:10.1029/WR022i001p00062

Paul F and 4 others (2004) Rapid disintegration of Alpine glaciers observed with satellite data. *Geophysical research letters* **31**(21). doi: 10.1029/2004GL020816

Paul F, Kääb A, Maisch M, Kellenberger T and Haeberli W (2004) Rapid disintegration of Alpine glaciers observed with satellite data. *Geophysical Research Letters* **31**(21). doi:10.1029/2004GL020816

Porter C and 10 others (2022) ArcticDEM-Strips, Version 4.1. *Harvard Dataverse*. doi:10.7910/DVN/C98DVS

Procházková B, Engel Z and Tomíček J (2019) Geometric changes of three glaciers in Dickson Land, central Spitsbergen, during the period 1990–2015. *Polar Science* **20**, 129–135. doi:10.1016/j.polar.2019.05.004

Promińska A, Cisek M and Walczowski W (2017) Kongsfjorden and Hornsund hydrography–comparative study based on a multiyear survey in fjords of west Spitsbergen. *Oceanologia* **59**(4), 397–412. doi:10.1016/j.oceano.2017.07.003

Przybylak R and 10 others (2014) Spatial distribution of air temperature on Svalbard during 1 year with campaign measurements. *International Journal of Climatology* **34**(14), 3702–3719. doi:10.1002/joc.3937

Rachlewicz G, Szczuciński W and Ewertowski M (2007) Post-"Little Ice Age" retreat rates of glaciers around Billefjorden in central Spitsbergen, Svalbard. *Polish Polar Research* **3**, 159–186.

RGI 7.0 Consortium (2023) *Randolph Glacier Inventory - A Dataset of Global Glacier Outlines, Version 7.0*. Boulder, Colorado USA. NSIDC: National Snow and Ice Data Center.

Rippin DM, Sharp M, Van Wychen W and Zubot D (2020) Detachment of icefield outlet glaciers: Catastrophic thinning and retreat of the Columbia Glacier (Canada). *Earth Surface Processes and Landforms* **45**(2), 459–472. doi:10.1002/esp.4746

Rowan AV and 7 others (2021) The role of differential ablation and dynamic detachment in driving accelerating mass loss from a debris-covered himalayan glacier. *Journal of Geophysical Research: Earth Surface* **126**(9), e2020JF005761. doi:10.1029/2020JF005761

Schauer U, Fahrbach E, Osterhus S and Rohardt G (2004) Arctic warming through the Fram Strait: Oceanic heat transport from 3 years of measurements. *Journal of Geophysical Research: Oceans* **109**(C6). doi:10.1029/2003JC001823

Schuler TV and 10 others (2020) Reconciling Svalbard glacier mass balance. *Frontiers in Earth Science* **8**, 156. doi:10.3389/feart.2020.00156

Serreze MC and Barry RG (2011) Processes and impacts of Arctic amplification: A research synthesis. *Global Planetary Change* **77**(1-2), 85–96. doi:10.1016/j.gloplacha.2011.03.004

Strzelecki MC and 6 others (2018) The role of rapid glacier retreat and landscape transformation in controlling the post-Little Ice Age evolution of paraglacial coasts in central Spitsbergen (Billefjorden, Svalbard). *Land Degradation & Development* **29**(6), 1962–1978. doi:10.1002/ldr.2923

Strzelecki MC, Szczuciński W, Dominiczak A, Zagórski P, Dudek J and Knight J (2020) New fjords, new coasts, new landscapes: The geomorphology of paraglacial coasts formed after recent glacier retreat in Brepollen (Hornsund, southern Svalbard). *Earth Surface Processes and Landforms* **45**(5), 1325–1334. doi:10.1002/esp.4819

van Pelt WJ, Schuler TV, Pohjola VA and Pettersson R (2021) Accelerating future mass loss of Svalbard glaciers from a multi-model ensemble. *Journal of Glaciology* **67**(263), 485–499. doi:10.1017/jog.2021.2

Wendler G (1975) A note on the advection of warm air towards a glacier. A contribution to the International Hydrological Decade. *Zeitschrift Für Gletscherkunde Und Glazialgeologie* **10**, 199–205.